Theoretical and experimental study of the scattering of photons by K-shell bound electrons: Energy and angular dependence of the cross sections

M. Pradoux, H. Meunier, M. Avan, and G. Roche
Laboratoire de Physique Nucléaire, Université de Clermont, Boîte Postale 45,63170 Aubiere, France
(Received 7 February 1977)

We present an analytic calculation of the differential cross section $d^2\sigma/d\Omega_{\vec{k}_f}d\omega_f$ using relativistic wave functions for the initial (s wave only) and final electron states. Comparisons are made with other theoretical calculations. Experimental results are given as a test of the theoretical calculation: energy spectra for 662-keV γ rays scattered incoherently through 90° and 135° by Ge bound electrons, and for 60-keV photons scattered by Cu and Mo K-shell electrons through 50°. Good agreement has been obtained between experimental and theoretical results.

I. INTRODUCTION

In these last years, there has been a resurgence of interest in photon scattering for energies less than 5 MeV. Two types of developments are now possible: numerical cross-section calculations with high-speed electronic computers and high-resolution measurements of γ-ray energies using Li-drifted germanium detectors. Experimental energy distributions[1] and theoretical differential cross sections have been studied

In the conventional photon scattering description, the electron is taken to be free. Indeed, this is an approximation because, in most cases, the electron is initially bound in an atom, which we consider here.

Until now, theoretical investigations on the incoherent scattering of photons by atomic electrons have been essentially nonrelativistic. They are based on the form-factor approximation ($\vec{p}\cdot\vec{A}$ terms dropped, where $\vec{p}$ is the electron momentum and $\vec{A}$ the vector potential of the electromagnetic radiation),[2] or the incoherent scattering approach,[3,4] or the impulse approximation.[5]

Subsequently, Randles,[6] Lambert *et al.*[7] and Schumacher[8] have used relativistic wave functions in evaluating the scattering form factor. Whittingham[9] has numerically calculated the differential cross section for the incoherent scattering of 662-keV γ rays by Pb K-shell electrons. This theory is relativistic and without any Hamiltonian approximation.

Eisenberger and Platzman[5] have estimated the importance of the $\vec{p}\cdot\vec{A}$ term in the coupling Hamiltonian

$$H_c = \frac{e^2A^2}{2mc^2} - e\,\frac{\vec{p}\cdot\vec{A}}{mc^2}\,,$$

and the importance of the relativistic correction. They have shown that the $\vec{p}\cdot\vec{A}$ correction term can be written

$$\delta^{\vec{p}\cdot\vec{A}} = (E_i/mc^2)^{1/2}\sin^{3/2}(\tfrac{1}{2}\theta)\,,$$

where E_i is the binding energy of the atomic electron and θ the scattering angle. The relativistic correction is given as

$$\delta^R = (\omega_i/mc^2)^{1/2}\sin^2(\tfrac{1}{2}\theta)\,,$$

where ω_i is the initial photon energy.

For 662-keV photons scattered through 90°, the formulas above show that $\delta^R \gg \delta^{\vec{p}\cdot\vec{A}}$. Our calculation presented herein then introduces the relativistic wave functions of Rose,[10] which take into account the electron binding for the initial discrete electron state and the Coulomb effect for the final state, while $\vec{p}\cdot\vec{A}$ terms are dropped in the coupling Hamiltonian. A comparison is made with existing theoretical results.

On the other hand, the disagreement between the results of recent scattering measurements of medium-energy γ rays[3,4,11,12] confirms the need for new measurements. Also, energy distributions of photons scattered inelastically have never been obtained.

As indicated in our preliminary paper,[1] the aim of our experimental study concerns the energy and angular distributions. We present herein results for the scattering of 662-keV photons by Ge K-shell electrons and of 60-keV photons by Cu and Mo K-shell electrons.

In Sec. II, the theoretical calculation is presented. Numerical results are examined and compared to other data in Sec. III. In Sec. IV, experimental results are given and comparison is made with the calculated values.

II. EXPRESSION OF THE CROSS SECTION

In the approximation in which $\vec{p}\cdot\vec{A}$ terms are dropped in the coupling Hamiltonian, the differential cross section for the scattering of a photon by a bound atomic electron is

$$\frac{d^3\sigma}{d\omega_f\, d\Omega_{\vec{k}_f}\, d\Omega_{\vec{p}_f}} = \frac{r_0^2}{(2\pi)^3}\,(\vec{e}_i\cdot\vec{e}_f)^2\,\frac{\omega_f}{\omega_i}\,p_f\,W_f\,|M|^2\,,$$

with ω_i and ω_f being the initial and final photon energy, $\vec{e}_i$ and $\vec{e}_f$ the corresponding polarization vectors, $\vec{k}_i$ and $\vec{k}_f$ the wave vectors of the incident and scattered waves, $\vec{p}_f$ and W_f the momentum and total energy of the final electron, and E_i and W_i the binding and total energy of the atomic electron.

The matrix element is expressed by

$$M=\int \Phi_f^*\, e^{i\Delta\vec{k}\cdot\vec{r}}\Phi_i\, d^3r\,,$$

with $\Delta\vec{k}=\vec{k}_i-\vec{k}_f$ and $\vec{r}$ the coordinate from the center of the atomic nucleus.

As indicated in the Introduction, relativistic electron wave functions are used. We introduce Rose's[10] wave functions, which are computed for hydrogenic atoms and expressed as a partial-wave series:

$$\Phi_i=\psi^{\mu_1}_{-1}$$

for the initial bound state, and

$$\Phi_f=4\pi\left(\frac{\pi}{2W_fp_f}\right)^{1/2}\times\sum_{k_2\mu_2}s_{k_2}\,C_{m_2'}(i)^{l_2}C(l_2,\tfrac{1}{2},j_2;\,\mu_2-m_2',m_2')\times Y^{*\mu_2-m_2'}_{l_2}(\hat{p}_f)\,\psi^{\mu_2}_{k_2}$$

for the final continuum state, with

$$\psi^{\mu}_{k}=\begin{pmatrix} g(r) & \chi^{\mu}_{k}(\hat{r}) \\ if(r) & \chi^{\mu}_{-k}(\hat{r})\end{pmatrix},$$

where the symbol k is a quantum number which combines j and the parity

$$k=\pm(j+\tfrac{1}{2})\quad\text{for } j=l\pm\tfrac{1}{2}$$

(k corresponds to $s_{1/2},p_{1/2},p_{3/2},\ldots$ states), and

$$C_{m_2'}C^*_{m_2'}=1\,,\quad s_{k_2}=\exp(i\pm\delta'_{k_2})\,,$$

δ'_{k_2} being the phase characteristic of the Coulomb field.

The wave functions Ψ^{μ}_{k} are solutions of the Dirac equation $H\Psi=W\Psi$, where $W=1+E$ is the total energy of the electron.

The spherical spinor $\chi^{\mu}_{k}(\hat{r})$ is an eigenstate of J^2 and L^2 (with J the angular momentum operator and L the orbital momentum operator):

$$\chi^{\mu}_{k}(\hat{r})=\sum_m C(l,\tfrac{1}{2},j;\,\mu-m,m)\,Y_l^{\mu-m}(\hat{r})\chi^m\,,$$

$C(j,j',j'';m'-m,m)$ being the Clebsch-Gordan coefficient,[13] $Y^m_l(\hat{r})$ the spherical harmonic, and χ^m the two-component Pauli spinor. The radial functions f and g are solutions of the equations

$$\frac{dg}{dr}=(W+1-V)f-\frac{(k+1)g}{r}\,,$$

$$\frac{df}{dr}=-(W-1-V)g+\frac{(k-1)f}{r}\,.$$

The cross section is obtained by inserting Φ_i and Φ_f into M:

$$M=4\pi\,\frac{\pi}{2W_fp_f}\int_r\sum_{\substack{L\\ k_2\mu_2}} i^L[4\pi(2L+1)]^{1/2}j_L(\Delta\vec{k}\cdot\vec{r})s^*_{k_2}C_{m_2'}(-i)^{l_2}C(l_2,\tfrac{1}{2},j_2;\,\mu_2-m_2',m_2')\,Y^{\mu_2-m_2'}_{l_2}(\hat{p}_f)\times\left\{g_1g^*_2\int_{\Omega_r}Y^0_L(\hat{r})\chi^{\mu_1}_{-1}\chi^{*\mu_2}_{k_2}\,d\Omega_r+f_1f^*_2\int_{\Omega_r}Y^0_L(\hat{r})\chi^{\mu_1}_{1}\chi^{*\mu_2}_{-k_2}\,d\Omega_r\right\}r^2\,dr\,.$$

We must calculate two angular integrals of the type

$$\int Y^m_l Y^{m'}_{l'}Y^{m''}_{l''}\,d\Omega$$

[for example, the solution of the first one is $\int Y^0_L(\hat{r})Y_0^{\mu_1-m}(\hat{r})Y^{*\mu_2-m}_{l_2}(\hat{r})\,d\Omega_r=1/(4\pi)^{1/2}$] and four radial integrals of the type[14]

$$\int_0^\infty r^{b-1}e^{-sr}F(a;c;t/r)=\Gamma(s)s^{-b}F(a,b;c;t/s)\,,$$

which transform a confluent hypergeometric function into a normal hypergeometric function.[15]

Then, M is written

$$M=4\pi\left(\frac{\pi}{2W_fp_f}\right)^{1/2}\sum_{k_2}s^*_{k_2}\,C_{m_2'}\,C(l_2,\tfrac{1}{2},j_2;\,\mu_1-m_2',m_2')\,Y^{\mu_1-m_2'}_{l_2}(\hat{p}_f)\,|k_2|^{1/2}\,\frac{(2p_f)^{\gamma_2-1/2}\Gamma(\delta)}{\Gamma(c)}\times\sum_0^{l_2}\frac{(l_2+n)!}{(l_2-n)!\,n!}\left(\frac{1}{2\Delta k}\right)^{n+1}[V'-i\epsilon V^n]$$

with

$$\epsilon = \left(\frac{1-W_i}{1+W_i}\right)^{1/2}\left(\frac{W_f-1}{W_f+1}\right)^{1/2}$$

$$V' = 2\Gamma(b)\,\mathrm{Re}(G+G'), \quad G = \beta\gamma'^{*}\gamma''F',$$

$$V'' = 2\Gamma(b)\,\mathrm{Im}(G-G'), \quad G' = \beta\gamma'\gamma''F,$$

$$\beta = i^{l_2+1-n}, \quad \delta = \gamma_2 + iy_2,$$

$$\gamma' = e^{-in}\delta^{*}, \quad b = \gamma_1+\gamma_2-n,$$

$$\gamma'' = [\lambda + i(\Delta k + p_f)]^{-b}, \quad c = 2\gamma_2+1,$$

n being the principal quantum number,

$$\chi = \frac{2ip_f}{\lambda + i(\Delta k + p_f)}, \quad F = F(\delta, b; c; \chi),$$

$$\lambda = \alpha Z, \quad F' = F(\delta+1, b; c; \chi),$$

$$\gamma_1 = (1+\lambda^2)^{1/2}, \quad y_2 = \lambda\, W_f/p_f,$$

$$\gamma_2 = (k_2^2-\lambda^2)^{1/2}, \quad e^{2i\eta} = -(k_2 + i\gamma_2/W_f)/\delta.$$

After summation over spins, integration over the direction of $\vec{p}_f$, and averaging on polarization states, we find for the scattering cross section of a photon by a K-shell electron

$$\frac{d^2\sigma}{d\Omega_{\vec{k}_f}\,d\omega_f} = r_0^2\,\frac{1+\cos^2\theta}{8\pi}\,\frac{(2\lambda)^{2\gamma_1+1}}{\Gamma(2\gamma_1+1)}\,(W_i+1)\,\frac{\omega_f}{\omega_i}\,e^{\pi y_2}(W_f+1)$$

$$\times \sum_{k_2} |k_2|\,\frac{(2p_f)^{2\gamma_2-1}\,|\Gamma(\gamma_2+iy_2)|^2}{[\Gamma(2\gamma_2+1)]^2}\left|\sum_{n=0}^{l_2}\frac{(l_2+n)!}{(l_2-n)!\,n!}\left(\frac{1}{2\Delta\kappa}\right)^{n+1}[V'-i\epsilon V'']\right|^2.$$

The differential cross section is expressed as an infinite series in k_2. This series is truncated when the radial integrals have decreased sufficiently.

To obtain the nonrelativistic limit from the relativistic differential cross section above, it is necessary to set W_i equal to 1 ($Z^2\alpha^2$ is neglected compared to unity so that $\gamma_2 = k_2$ and $\epsilon = 0$). Then $f(r)$ vanishes and $g(r)$ becomes the nonrelativistic radial function. This procedure requires a different computer program.

III. THEORETICAL RESULTS

The numerical calculation of the cross section has been performed using a CDC 6600 computer. A separate numerical computation of the cross section is necessary for each choice of photon energy and atomic number, which increases the amount of computer time. The main difficulty in the calculation is connected with the hypergeometric functions. For a given incident energy value, the hypergeometric functions are calculated from the series expansion when the final photon energy is greater than the free-electron value, while an analytical continuation must be used for smaller final energies. The convergence of the sums becomes very slow for energies close to the free-case value.

The results obtained for a photon energy $\omega_i = 662$ keV, scattering angles $\theta = 50°$, 70°, 90°, 135°, and $Z = 32$ (germanium) are presented in Fig. 1 as a function of the final electron energy for comparison to experiment. The maximum of the spectrum is shifted from the free-electron scattering energy. This shift is minimal and equal to 15 keV for $\theta = 90°$, and it increases to 30 keV for lower and larger scattering angles. The full width at half maximum (FWHM) is maximal and equal to 90 keV for $\theta = 70°$; it decreases to 50 keV for smaller and larger scattering angles. In this figure, we give also a nonrelativistic result for $\theta = 90°$ which is very different from the relativistic case (nonrelativistic result: FWHM = 110 keV; relativistic result: FWHM = 75 keV). The maximum of the nonrelativistic spectrum is shifted from the rela-

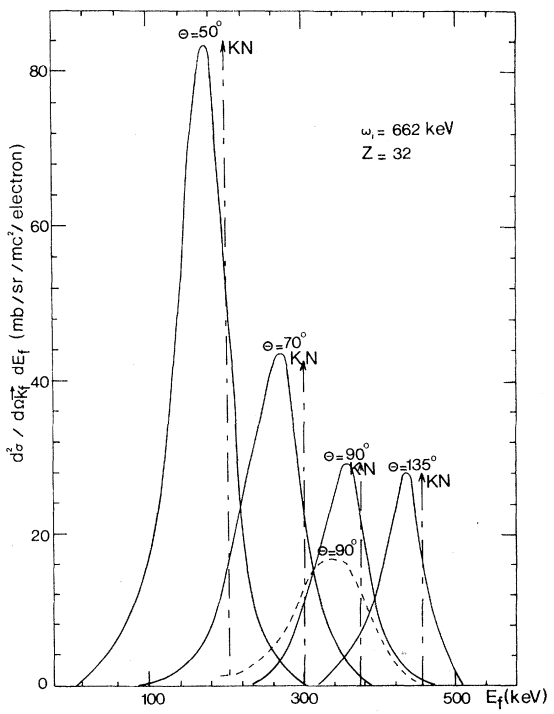

FIG. 1. Scattering cross section $d^2\sigma/d\Omega_{\vec{k}_f}\,dE_f$ as a function of the electron kinetic energy E_f: ——, present work (relativistic calculation); ----, present work (nonrelativistic calculation); KN, energy value for the scattering by free electrons.

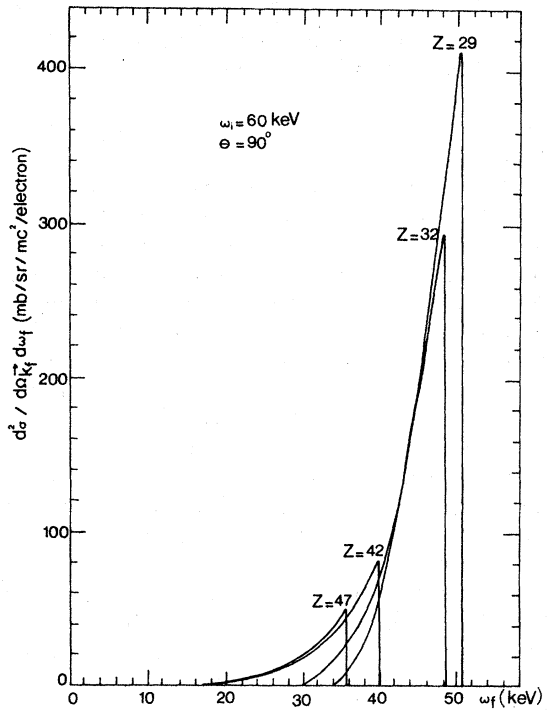

FIG. 2. Scattering cross section as a function of the final photon energy. The numbers attached to the curves give the atomic numbers of the target elements (Cu, $Z=29$; Ge, $Z=32$; Mo, $Z=42$; Ag, $Z=47$).

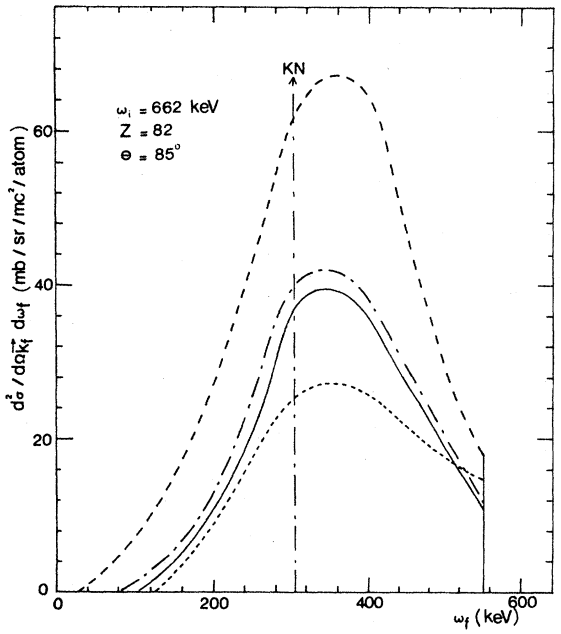

FIG. 3. Scattering cross section $d^2\sigma/d\Omega_{k_f} d\omega_f$ vs photon energy for a primary energy of 662 keV. A comparison between our results and Schumacher and Whittingham's ones: ——, present work (relativistic calculation); ----, present work (nonrelativistic calculation); ———, Schumacher's calculation (Ref. 8); — — —, Whittingham's calculation (Ref. 9).

tivistic one by 15 keV.

In Fig. 2, energetic distributions in the case $\omega_i = 60$ keV and $\theta = 90°$ are plotted for target atoms Cu, Ge, Mo, and Ag. The spectra are also shifted from the free-electron scattering energy, and they drop to zero abruptly at the K-shell energy limit. The shift is proportional to Z and equal to the binding energy of the electron. The FWHM is constant and equal to 6 keV.

A comparison of theoretical scattering profiles is made for existing results of the differential cross section $d^2\sigma/d\Omega_{k_f} d\omega_f$ (Figs. 3–6). The position of the maximum of the spectrum for our relativistic calculation (relativistic present work) agrees with other relativistic results (Whittingham[9] and Schumacher[8]), but not with Gavrila's[16] and Schnaidt's[2] nonrelativistic results. The FWHM of all nonrelativistic spectra (310 keV) are larger than those for relativistic spectra (250 keV). Our relativistic results fit very well to Schumacher's,

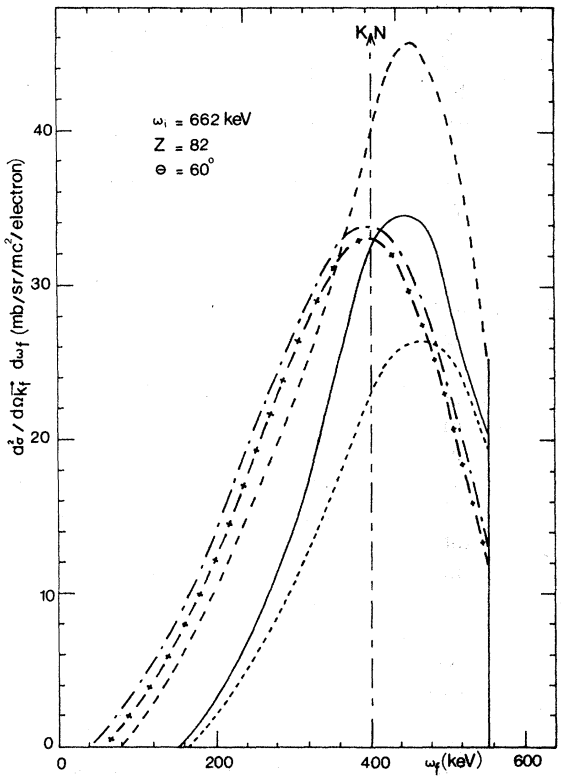

FIG. 4. Scattering cross section $d^2\sigma/d\Omega_{k_f} d\omega_f$ vs photon energy for a primary energy of 662 keV. A comparison between our results and other published ones: ——, present work (relativistic calculation); -----, present work (nonrelativistic calculation); — — —, Whittingham's calculation (Ref. 9); -.-.-, -.-.-.-, Hamiltonian $A^2 + \vec{p}\cdot\vec{A}$ [Gavrila's calculation, reported by Tseng *et al.*, (Ref. 16)]; +−+−, Hamiltonian A^2 [Schnaidt's calculation, reported by Tseng *et al.* (Ref. 16)].

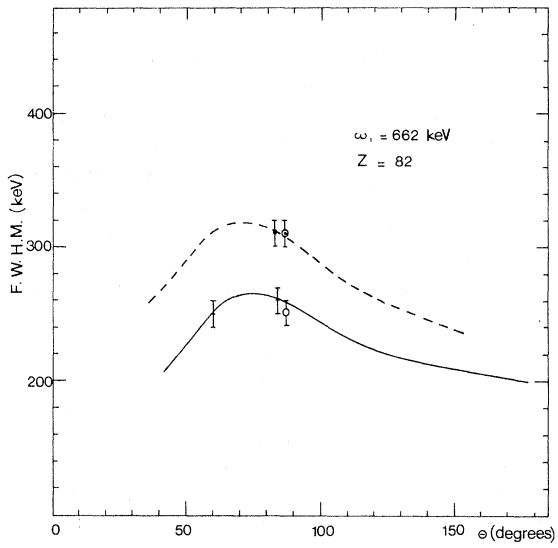

FIG. 5. Full width at half maximum of bound spectrum as a function of the scattering angle Θ: ——, present work (relativistic calculation); ----, present work (nonrelativistic calculation); Ī , Whittingham's calculation (Ref. 9) (relativistic); Ō , Schumacher's calculation (Ref. 8) (relativistic); Ī , Schnaidt's calculation (Ref. 16) (nonrelativistic); Ō , Gavrila's calculation (Ref. 16) (nonrelativistic).

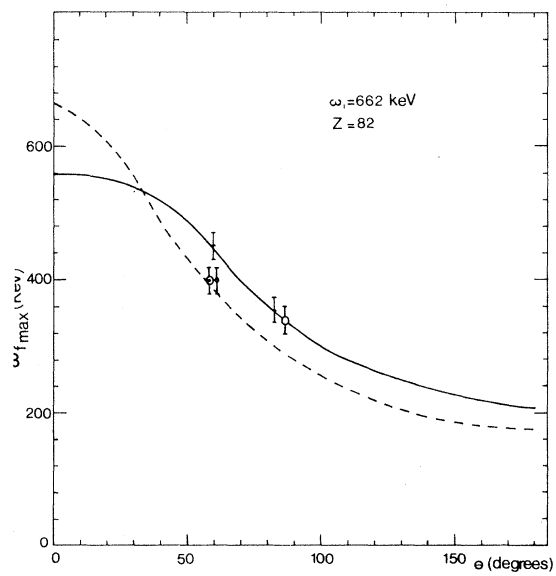

FIG. 6. Energy of the maximum of the bound spectrum and energy of the scattered photon in the free scattering case as a function of the scattering angle Θ: – – –, free-electron case. Bound-electron theory: ——, present work (relativistic calculation); Ī , Whittingham's calculation (Ref. 9) (relativistic); Ō , Schumacher's calculation (Ref. 8) (relativistic); Ī , Schnaidt's calculation (Ref. 16) (nonrelativistic); Ō , Gavrila's calculation (Ref. 16) (nonrelativistic). For a given angle value, the difference between the curves gives the shift of the maximum.

while a discrepancy of 50% to 100% in the amplitudes of the distributions must be pointed out between Whittingham's and other relativistic calculations.

Angular distributions ($d\sigma/d\Omega_{\vec{k}_f}$) are presented in Fig. 7 ($\omega_i = 662$ keV) and Fig. 8($\omega_i = 60$ keV). Our calculation and Whittingham's results are similar in shape (Fig. 7). Nevertheless, it can be seen that Whittingham's values are higher than ours (50% to 100% as indicated above). For small scattering angles, the behavior of the distributions in both cases, free initial electron and bound initial electron, is very different. The effect of the electron binding gives a decrease of the cross section at small angles, while the Klein-Nishina cross section increases to a higher value at $\theta = 0°$. Gavrila's nonrelativistic and impulse-approximation[16] calculations yield higher values of the cross section compared to our relativistic calculation at angles less than 60°.

For incident photons of 60 keV, there are no other theoretical results (to our knowledge). Figure 8 shows that the bound-electron results are in complete disagreement with the free-electron curve.

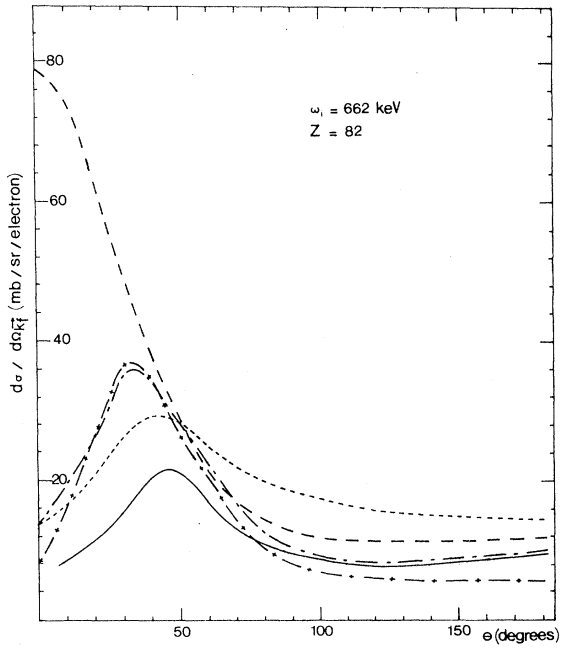

FIG. 7. Scattering cross section $d\sigma/d\Omega_{\vec{k}_f}$ as a function of the scattering angle Θ. A comparison between different theoretical results. Free-electron scattering: – – –, Klein-Nishina calculation. Bound-electron scattering: ——, present work (relativistic calculation); -----, Whittingham's calculation (Ref. 9); -----, Hamiltonian $A^2 + \vec{p}\cdot\vec{A}$ [Gavrila's calculation (Ref. 16)]; +— +—, impulse-approximation calculation (Ref. 16).

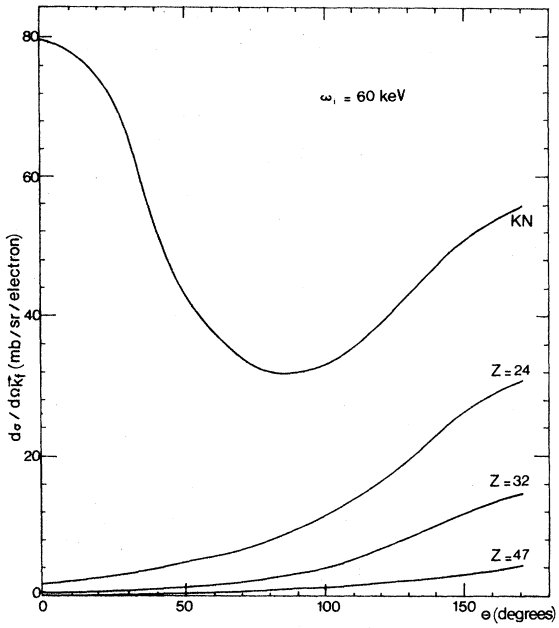

FIG. 8. Scattering cross section $d\sigma/d\Omega_{\vec{k}_f}$ as a function of the scattering angle Θ: KN, free-electron scattering; $Z = 24$, 32, 47, bound-electron scattering.

A comparison between theoretical angular distributions and experimental results[3,12,17] at 662 keV ($Z = 82$) is made in Fig. 9. We give our relativistic angular distribution, Whittingham's, and impulse-approximation ones for comparison with Sujkowski and Nagel,[3] East and Lewis,[12] and Pingot's[17] experimental results. Our relativistic distribution fits the experimental results better than Whittingham's one. The behavior of the nonrelativistic impulse-approximation distribution is in complete disagreement with both relativistic theories and experimental results.

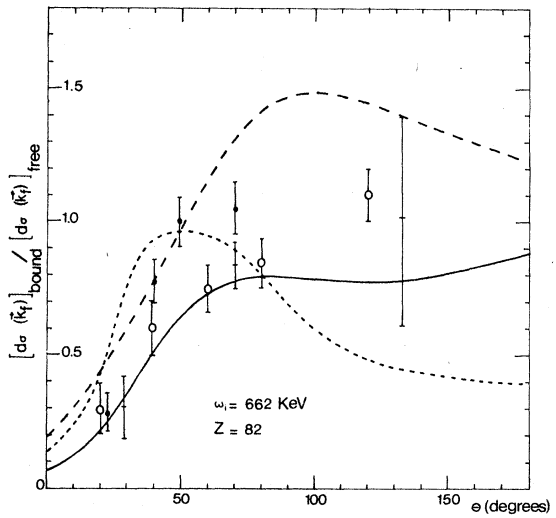

FIG. 9. Angular dependence of cross-section ratio $[d\sigma(\vec{k}_f)]_{\text{bound}} / [d\sigma(\vec{k}_f)]_{\text{free}}$ for scattering of 662-keV photons. Theoretical dependence: ——, present work (relativistic calculation); -----, Whittingham's calculation (Ref. 9) (relativistic); ....., impulse approximation (Ref. 16) (nonrelativistic). Experimental results: ⧱, Sujkowski and Nagel (Ref. 3); ⧱, Pingot (Ref. 17); ⧱, East and Lewis (Ref. 12).

IV. EXPERIMENTAL RESULTS

We have measured the differential scattering cross section and hence the scattering profile. Scattering experiments were performed on germanium K-shell electrons using 662-keV γ rays (^{137}Cs source of 86 mCi) and on Cu and Mo bound electrons using 60-keV photons (^{241}Am source of 100 mCi).

The experimental setup described in Ref. 1 allows a study of the 662-keV photons incoherently scattered on Ge K-shell electrons. The target is a thin slice of Ge crystal which is also used as electron detector. The use of a high-resolution detector allows a better discrimination against background and a detailed study of the scattered γ-ray spectra. Data were taken in two separate runs of about 450 and 300 h, respectively.

For the experiment with the ^{241}Am radioactive source, the scattered photon detector (D) is the Ge(Li) crystal mentioned above and the target a thin slice of Cu or Mo (Fig. 10). With this setup, we can measure chance events which are not negligible. In the present investigation, the counters were shielded in such a manner than they cannot see γ or x rays scattered from one crystal to another.

Figure 11 gives the experimental scattering profile of 662-keV photons scattered at $\theta = 90°$ by K-shell electrons of Ge. The energy spectrum of the recoil electron is given in Figs. 12 and 13 for $\theta = 90°$ and 135°. These experimental results are compared with our theoretical calculations (relativistic case: solid lines; nonrelativistic case: dotted lines). The areas under the curves of both experimental spectra and theoretical relativistic

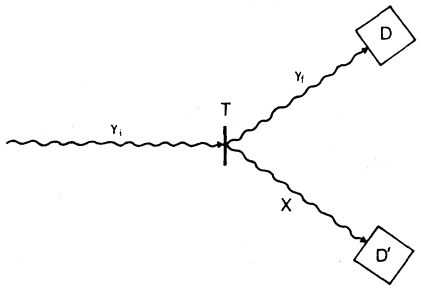

FIG. 10. Detectors arrangement using an external target T for the experiment with a ^{241}Am source. Detector D: Ge(Li) crystal; detector D': NaI(Tl) crystal.

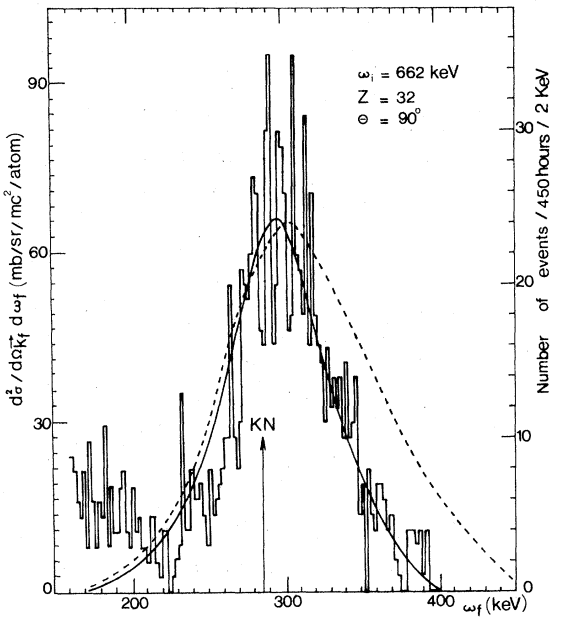

FIG. 11. Comparison between our theoretical photon energy spectrum as a function of the final photon energy and experimental results (arrangement described in Ref. 1). The experimental number of events corresponds to the solid angle defined by the γ-ray detector: ——, relativistic calculation; -----, nonrelativistic calculation.

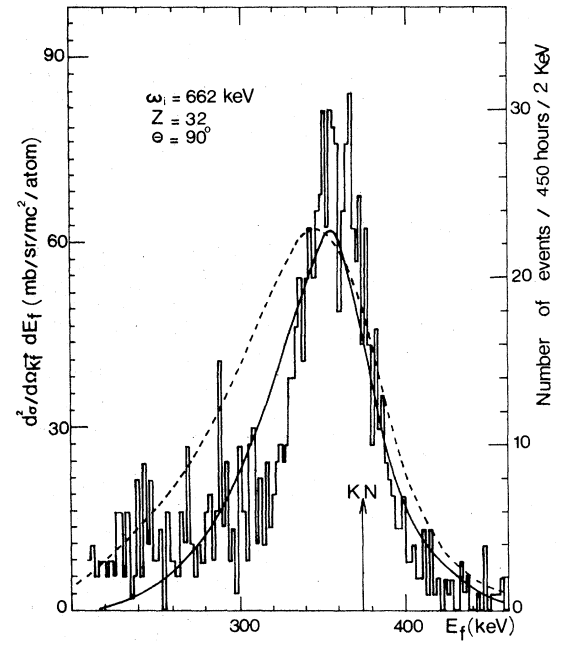

FIG. 12. Comparison between our theoretical electron energy spectrum as a function of the final electron energy and experimental results (arrangement described in Ref. 1) for $\Theta = 90°$: ——, relativistic calculation; -----, nonrelativistic calculation.

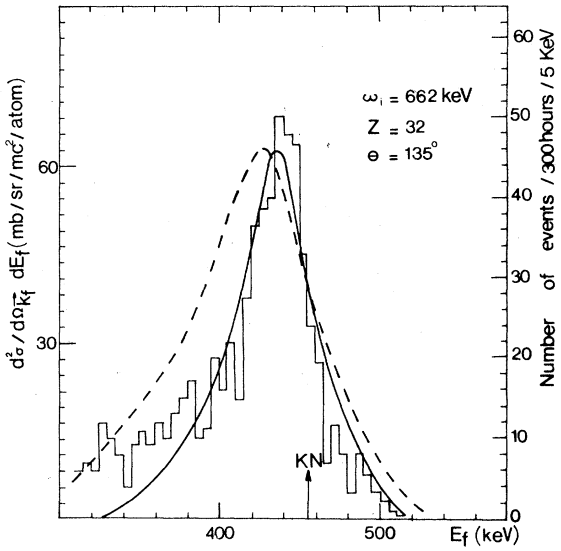

FIG. 13. Comparison between our theoretical electron energy spectrum as a function of the final electron energy and experimental results (arrangement described in Ref. 1) for $\Theta = 135°$: ——, relativistic calculation; -----, nonrelativistic calculation.

distributions are normalized. A good agreement is observed between the experimental spectra and the relativistic cross section calculated in the present work, while a discrepancy can be seen for the nonrelativistic calculation.

For the 662-keV incident photons and the germanium target ($Z = 32$), the FWHM of the theoretical relativistic distributions and experimental spectra as a function of the scattering angle θ is given in Fig. 14. We show also (Fig. 15) the energy of the maximum of the bound spectrum and the energy of the recoil electron in the free-scat-

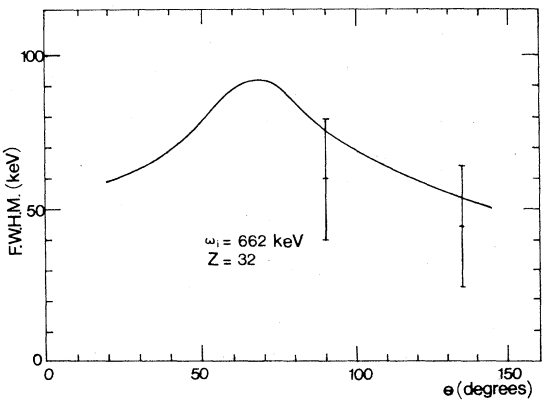

FIG. 14. Full width at half maximum of the theoretical and experimental distributions as a function of the scattering angle Θ: ——, theoretical relativistic distribution (present work); I, experimental results (present work).

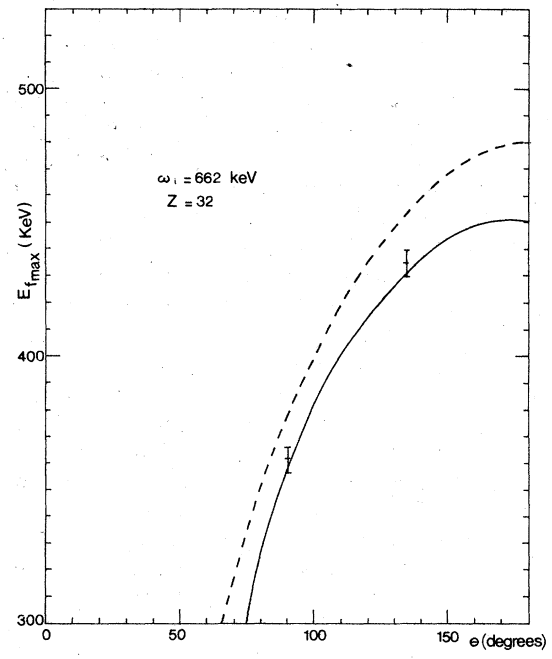

FIG. 15. Energy of the maximum of the bound spectrum and energy of the recoil electron in the free scattering case as a function of the scattering angle Θ: – – –, free-electron case. Bound-electron case: ——, theoretical relativistic distribution (present work); I, experimental results (present work).

tering case as a function of the scattering angle θ (theoretical relativistic calculation and experimental results). The angular dependence of the cross-section ratio $[d\sigma(\vec{k}_f)]_{bound}/[d\sigma(\vec{k}_f)]_{free}$ is then given in Fig. 16 (theoretical and experimental results). In these figures (14–16), the agreement between our theoretical relativistic calculation and experimental results is indicated.

For 60-keV incident photons and Cu and Mo targets, the energetic distributions of the scattered photons on K-shell electrons are obtained from the total coincidence experimental spectrum by substracting chance coincidences (Figs. 17 and 18). The total coincidence spectrum for each target was stored during 140-h runs. Below the iodine x-ray line (32 keV), the main contribution arises from several x rays. Therefore, little information can be obtained from this part of the spectrum. The theoretical results for Cu and Mo are also plotted on the graphs (dotted lines). For these measurements, there are poor statistics. Nevertheless, agreement between the experimental and calculated scattering profiles can be seen.

In these experiments (662-keV and 60-keV incident photons), the coincidence rate is very low (about 0.05 event per hour). The correspondingly long measurement durations (many weeks) yield large experimental errors (for example, see Fig. 16).

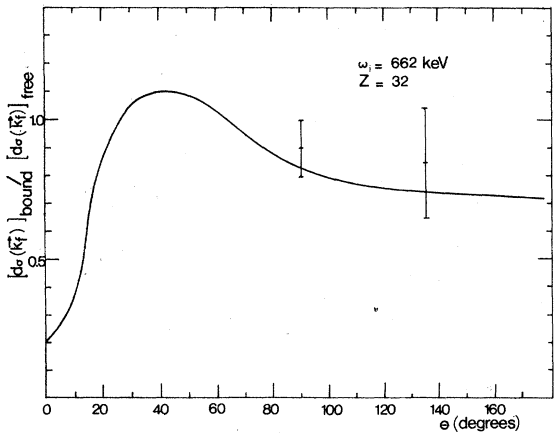

FIG. 16. Angular dependence of the cross-section ratio $[d\sigma(\vec{k}_f)]_{bound}/[d\sigma(\vec{k}_f)]_{free}$ for the scattering of 662-keV photons on Ge K-shell electrons: ——, theoretical relativistic distribution (present work); I, experimental results (present work).

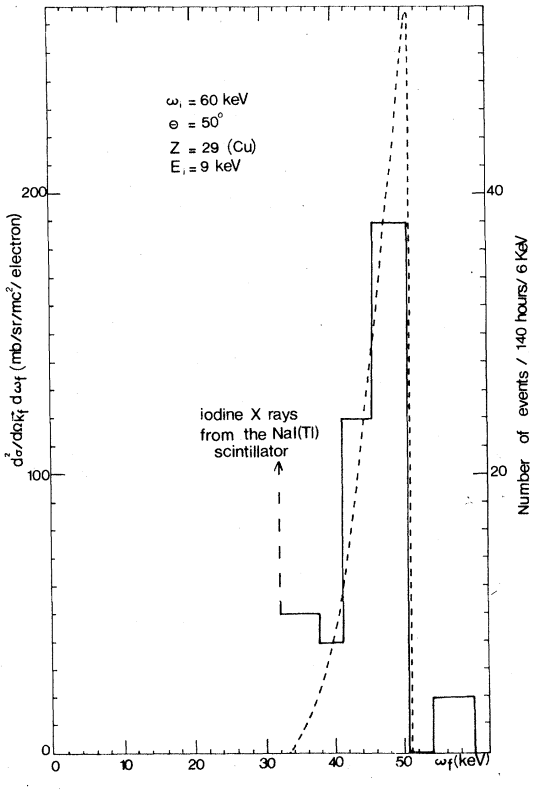

FIG. 17. Scattering experimental and theoretical spectra as a function of the final photon energy for a Cu target and 60-keV photons: ——, experimental profile (present work); -----, theoretical relativistic distribution (present work).

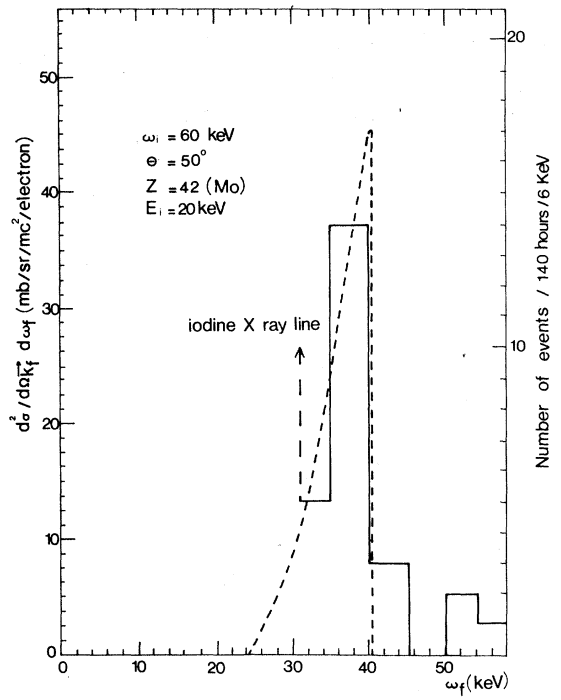

FIG. 18. Scattering experimental and theoretical spectra as a function of the final photon energy for a Mo target and 60-keV photons: ——, experimental profile (present work); -----, theoretical relativistic distribution (present work).

V. CONCLUSION

This theoretical and experimental study of the scattering of photons by K-shell bound electrons involves two main conclusions.

First, for 662-keV incident photons, we have tested the validity of our relativistic calculation by comparison with other theoretical calculations and with experimental results.

Our experimental arrangement with a triple coincidence technique (662-keV measurements) clarifies the confused situation existing for published double-coincidence results. The energy spectra of γ rays incoherently scattered by K electrons of Ge have been measured. The best statistical accuracy is therefore achieved here. We have found that the spectra are broadened compared to those obtained from scattering by free electrons. The maximum of the spectra appears at energies slightly larger than the energy for scattering by free electrons. We have measured energy shifts of 15 keV for $\theta = 90°$ and 20 keV for $\theta = 135°$. Furthermore, these energy shifts are found in the opposite direction to that obtained by Di Lazzaro and Missoni.[18]

The shifts and the FWHM of the experimental spectra are in agreement with our relativistic theoretical previsions. But, as would be expected, the nonrelativistic theory seems to give a poor description of the experimentally observed spectra.

The second conclusion concerns the study at 60 keV. To our knowledge, no study of the phenomenon has previously been performed at 60-keV incident photon energy.

In this paper, we have presented experimental spectra measured for inelastic scattering by K-shell electrons of Cu and Mo at an angle $\theta = 50°$. The incident photons of 60-keV energy are obtained from a ^{241}Am radioactive source.

The main features of the theoretical differential cross sections $d^2\sigma/d\Omega_{\vec{k}_f}\, d\omega_f$ calculated herein appear as an abrupt drop to zero at energy $\omega_f = \omega_i - E_i$ and a constant FWHM of 6 keV. These features are supported by the experimental energy spectra.

Both theoretical calculations and experimental results appear to be in complete disagreement with the Klein-Nishina theory.

ACKNOWLEDGMENTS

The authors wish to thank Professor L. Avan (CNAM, Paris) who suggested this study and Professor J. Proriol (University of Clermont-Ferrand) for his continued encouragements. They also like to thank Professor R. H. Pratt and L. D. Kissel (University of Pittsburgh) and Professor H. K. Tseng (University of Tai-Wan) for many valuable discussions and advice concerning the theoretical calculation. This work was supported in part by the NATO Science Committee (Research Grants Nos. 738 and 828.

[1]M. Pradoux, H. Meunier, J. Baumann, and G. Roche, Nucl. Instrum. Methods 112, 443 (1973).
[2]F. Schnaidt, Ann. Phys. (Leipz.) 21, 89 (1934).
[3]Z. Sujkowsky and B. Nagel, Ark. Phys. 20, 323 (1961).
[4]S. Shimizu, Y. Nakayama, and T. Mukoyama, Phys. Rev. 140, A806 (1965).
[5]P. Eisenberger and P. M. Platzman, Phys. Rev. A 2, 415 (1970).
[6]J. Randles, Proc. Phys. Soc. London A 70, 337 (1957).
[7]M. Lambert, R. Müller, J. Lang, R. Bösch, and W. Wölfli, Helv. Phys. Acta 39, 355 (1966).
[8]M. Schumacher, Z. Phys. 242, 444 (1971).
[9]I. B. Whittingham, J. Phys. A 4, 21 (1971).
[10]M. E. Rose, *Relativistic Electron Theory* (Wiley, New York, 1961).
[11]J. W. Motz and G. Missoni, Phys. Rev. 124, 1458

(1961).
[12]L. V. East and E. R. Lewis, Physica 44, 595 (1969).
[13]M. E. Rose, *Elementary Theory of Angular Momentum* (Wiley, New York, 1957).
[14]M. A. Abramowitz and I. A. Stegun, *Handbook of Mathematical Functions* (U.S. GPO, Washington, D. C., 1968).
[15]P. Appel and J. Kampé de Feriet, *Fonctions Hypergéométriques* (Gauthier-Villars, Paris, 1926).
[16]H. K. Tseng, M. Gavrila, and R. H. Pratt, University of Pittsburgh, Report No. 2, 1973 (unpublished).
[17]O. Pingot, Nucl. Phys. A 119, 667 (1968).
[18]M. A. Di Lazzaro and G. Missoni, Ann. Inst. Super. Sanita 1, 1 (1965).